

Lithium Diisopropylamide-Mediated Ortholithiations:  
Lithium Chloride Catalysis

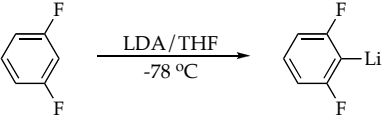
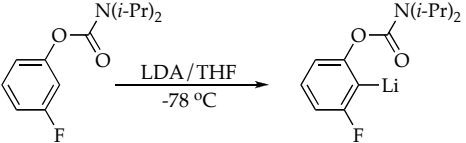
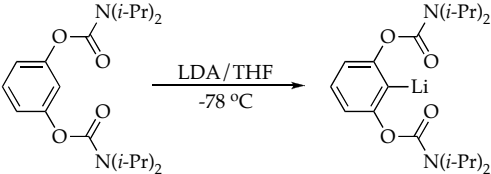
Lekha Gupta, Alexander C. Hoepker, Kanwal Jit Singh and David B. Collum\*

Contribution from the Department of Chemistry and Chemical Biology

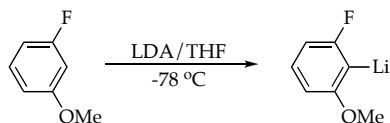
Baker Laboratory, Cornell University

Ithaca, New York 14853-1301

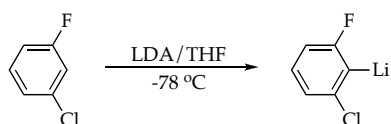
Supporting Information

	Page
<b>Experimental</b>	
<b>I</b> Measurement of chloride concentration using potentiometry and ion-chromatography	S6
<b>IR Rate Studies</b>	
<b>I</b> Representative in situ IR spectroscopic analysis of an ortholithiation	S7
<b>II</b> Plot of IR absorbances versus time for the ortholithiation of 1,3-difluorobenzene	S8
	
<b>III</b> Plot of IR absorbances versus time for the ortholithiation of 3-fluorophenyl- <i>N,N</i> -diisopropylcarbamate	S9
	
<b>IV</b> Plot of IR absorbances versus time for the ortholithiation of 1,3-bis( <i>N,N</i> -diisopropylcarbamoyl)benzene	S10
	

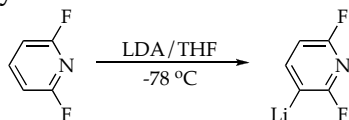
V Plot of IR absorbances versus time for the ortholithiation of 3-fluoroanisole S11



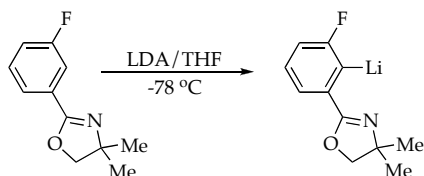
VI Plot of IR absorbances versus time for the ortholithiation of 1-chloro-3-fluorobenzene S12



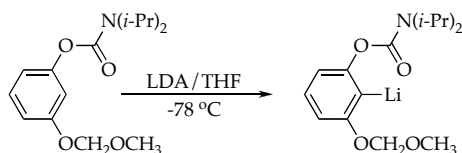
VII Plot of IR absorbances versus time for the ortholithiation of 2,6-difluoropyridine S12



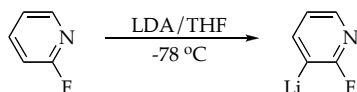
VIII Plot of IR absorbances versus time for the ortholithiation of 2-(3-fluorophenyl)-4,4-dimethyl-4,5-dihydro-1,3-oxazole S13



IX Plot of IR absorbances versus time for the ortholithiation of 3-methoxymethoxyphenyl-*N,N*-diisopropylcarbamate S14



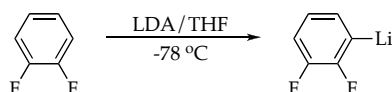
X Plot of IR absorbances versus time for the ortholithiation of 2-fluoropyridine S15



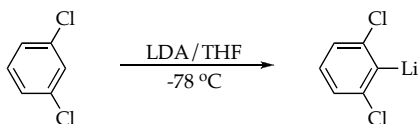
**XI** Plot of IR absorbances versus time for the ortholithiation of 1,4-difluorobenzene S16



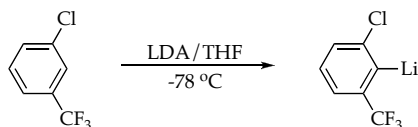
**XII** Plot of IR absorbances versus time for the ortholithiation of 1,2-difluorobenzene S17



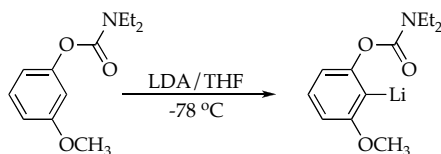
**XIII** Plot of IR absorbances versus time for the ortholithiation of 1,3-dichlorobenzene S18



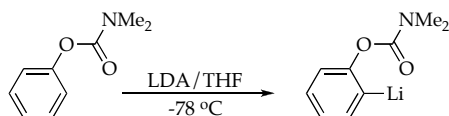
**XIV** Plot of IR absorbances versus time for the ortholithiation of 3-chlorobenzotrifluoride S19



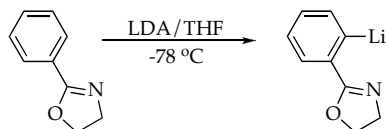
**XV** Plot of IR absorbances versus time for the ortholithiation of 3-methoxyphenyl-*N,N*-diethylcarbamate S20



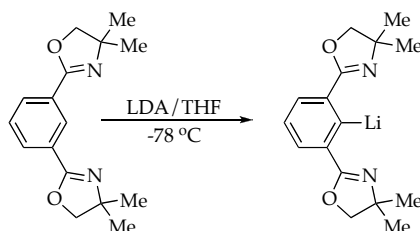
**XVI** Plot of IR absorbances versus time for the ortholithiation of phenyl-*N,N*-dimethylcarbamate S20



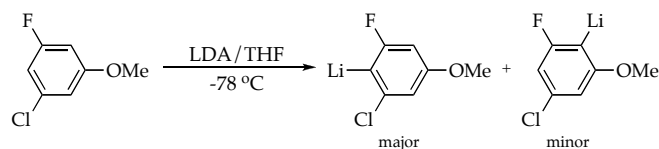
**XVII** Plot of IR absorbances versus time for the ortholithiation of 2-phenyl-2-oxazoline S21



**XVIII** Plot of IR absorbances versus time for the ortholithiation of 1,3-bis(4',4'-dimethyl-2'-oxazolinyl)benzene S22

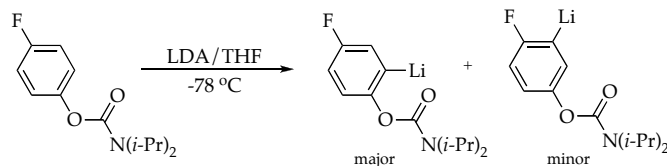


**XIX** Plot of IR absorbances versus time for the ortholithiation of 3-chloro-5-fluoroanisole S23



**XX** Plot of <sup>19</sup>F NMR peak integrations versus time for the ortholithiation of 3-chloro-5-fluoroanisole S23

**XXI** Plot of IR absorbances versus time for the ortholithiation of 4-fluorophenyl-*N,N*-diisopropylcarbamate S24



**XXII** Plot of <sup>19</sup>F NMR peak integrations versus time for the ortholithiation of *N,N*-diisopropyl-4-fluorocarbamate S24

**XXIII** Plot of IR absorbances versus time for the ortholithiation of 1,4-difluorobenzene in the presence of different lithium salts S25

**XXIV** Plot of IR absorbances versus time for the ortholithiation of 1,4-difluorobenzene using different sources of LDA S26

**Note:**

- 1) All reported LiCl mol percentages are with respect to [LDA].
- 2) Rates corresponding to the plots from **XV** to **XVIII** were determined at temperatures other than  $-78^{\circ}\text{C}$ .
- 3) Be aware of frequent changes in the scale on x-axis.

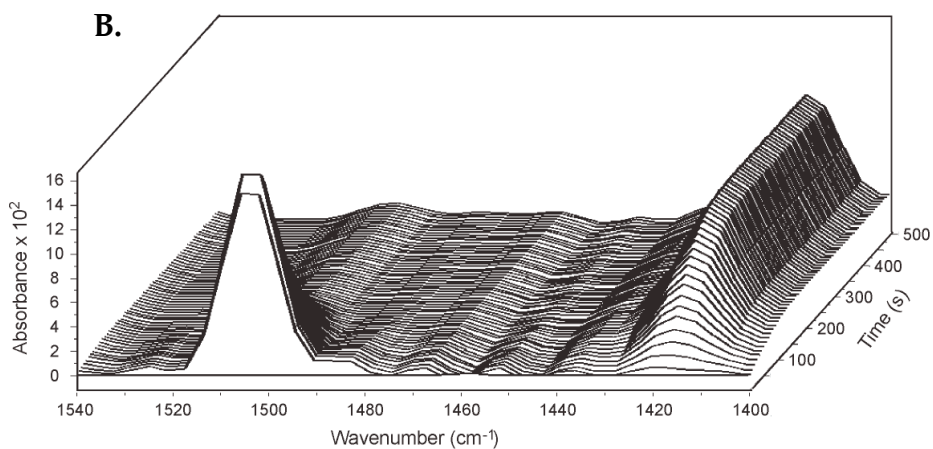
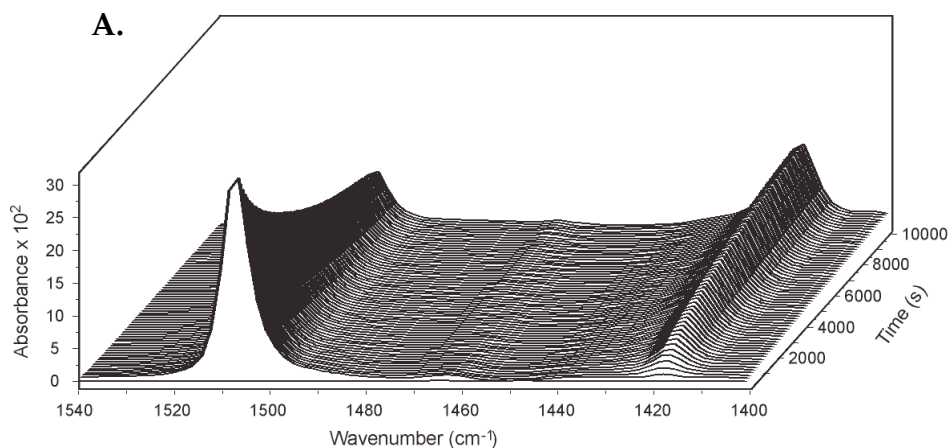
## Experimental

### I. Measurement of chloride concentration:

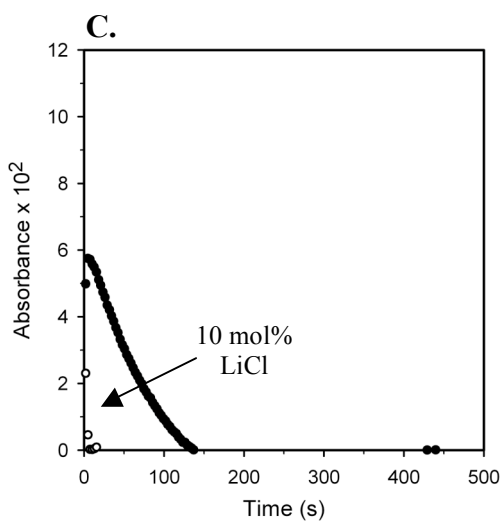
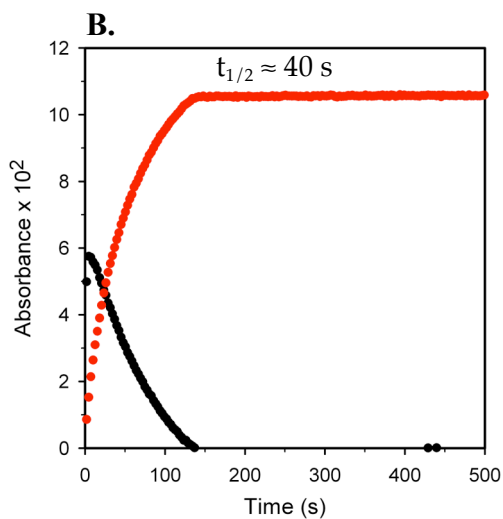
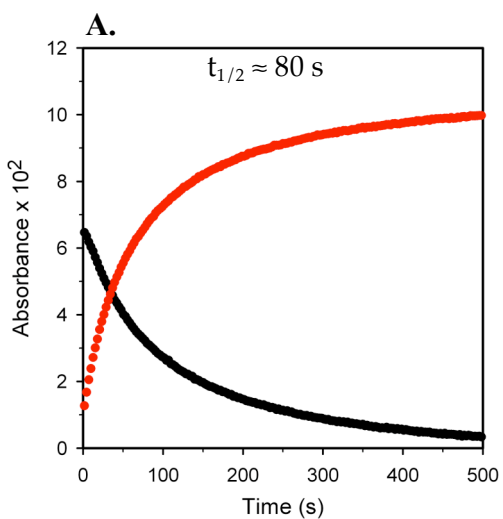
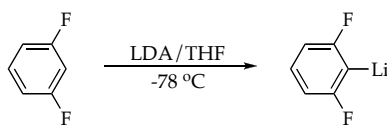
**Potentiometry:** The chloride concentration was determined potentiometrically by measuring the potential against a saturated potassium chloride solution. After calibrating with known concentrations of chloride, the concentration was calculated with the Nernst equation ( $E = E^\circ - (RT/zF) \log_{10} Q$ , where  $Q = [\text{Cl}^-]$ ;  $RT/zF$  is determined via calibration and is ideally 59.1 mV). The potential was measured with a potentiostat of low impedance. Both reference and indicating electrodes are made of silver plated with silver chloride (Ag/AgCl). Samples were prepared by quenching 25 mg of LDA or 100  $\mu\text{l}$  of 1.6 M *n*-BuLi with high-purity water (from Abruña group), evacuating to dryness and redissolving in water. Because the electrodes require a near neutral pH, the quenched base solutions needed to be neutralized with  $\text{HNO}_3$ . The LiCl standards were accordingly enriched with  $\text{NaNO}_3$  to ensure comparable activity. Both  $\text{HNO}_3$  and  $\text{NaNO}_3$  contained <0.5 ppm and <0.0003%  $\text{Cl}^-$ , respectively. The lower detection limit for  $\text{Cl}^-$  is approximately 0.5 ppm.

**Ion Chromatography:** Ion chromatography was performed on a Dionex ICS-2000 system (Sunnyvale, CA) with a Dionex Ionpac AG18 guard column and a Dionex Ionpac AS18 separation column. Samples and standards were run in the isocratic mode (1.0 ml/min) using 38 mM KOH as eluent. Elution time of chloride varied from 3.94 to 4.23 min. The suppression was achieved by a Dionex ASRS ULTRA II 4 mm self-regenerating suppressor. The column temperature was 30 °C and the working electric current was 100 mA. The eluent flow rate is 1.0 ml/min. The injection volume is 25  $\mu\text{l}$ . Samples were prepared by quenching 25 mg of LDA or 100  $\mu\text{l}$  of 1.6 M *n*-BuLi with high-purity water (from Abruña group), evacuating to dryness and redissolving in water. Aqueous samples of pH 12-13 were injected in duplicate into the chromatograph. The lower detection limit is approximately 10 ppb.

## IR Rate Studies

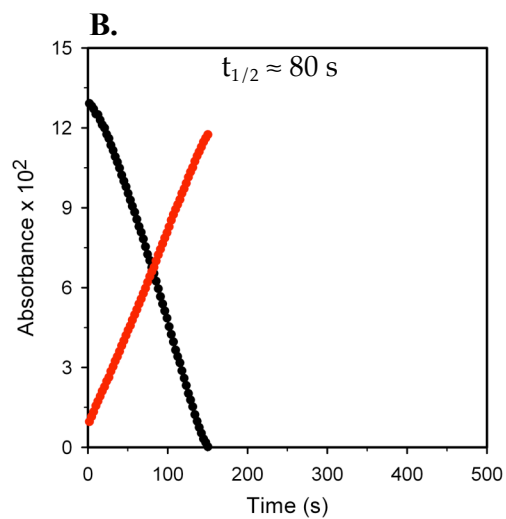
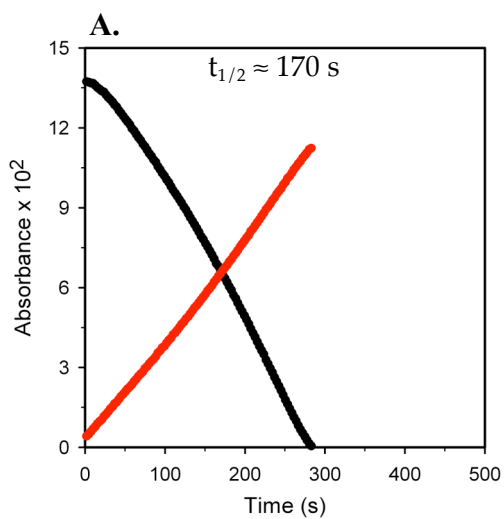
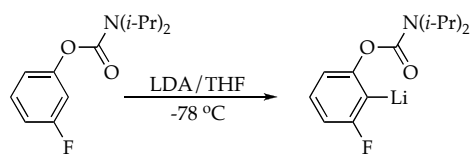


I. Representative in situ IR spectroscopic analysis of the ortholithiation of 1,4-difluorobenzene (0.1 M) with LDA (0.12 M) in neat THF at  $-78\text{ }^\circ\text{C}$ : (A) no added LiCl; (B) 0.5 mol % LiCl. The IR absorbance at  $1507\text{ cm}^{-1}$  corresponds to 1,4-difluorobenzene, whereas the absorbance at  $1418\text{ cm}^{-1}$  corresponds to its lithiated form.

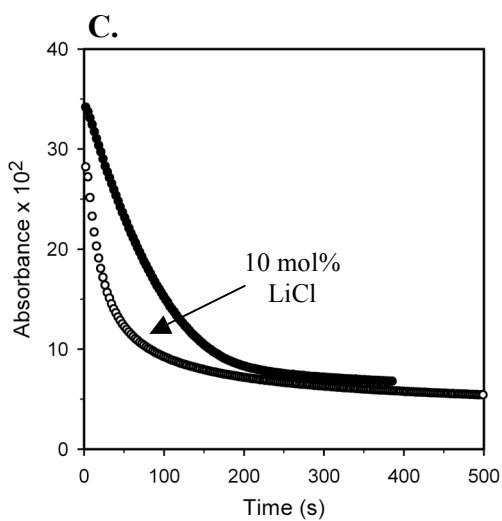
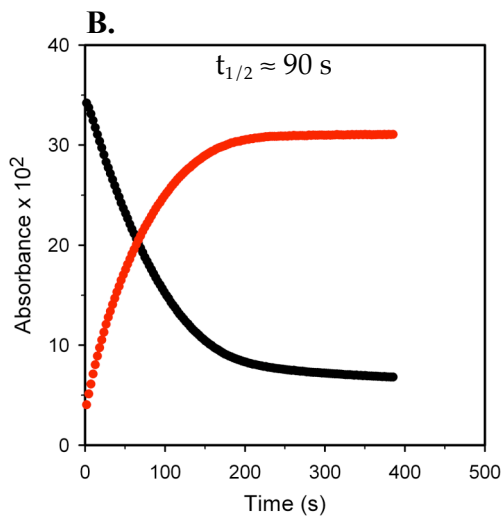
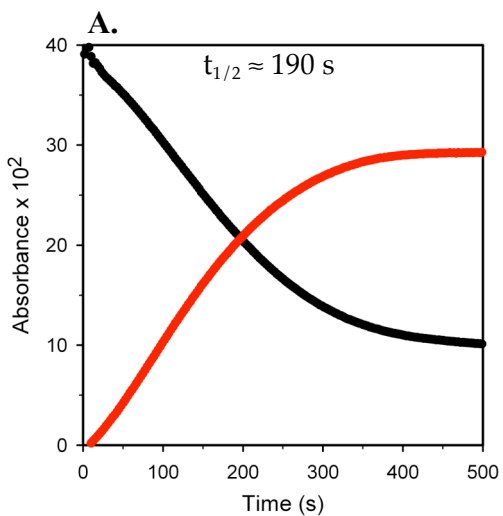
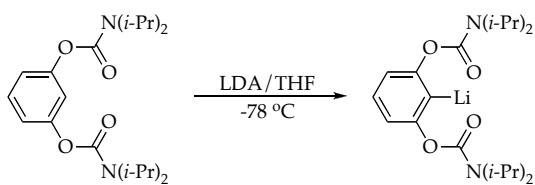


**II.** Plot of IR absorbances (black –  $1606\text{ cm}^{-1}$ , red –  $1406\text{ cm}^{-1}$ ) versus time for the ortholithiation of 1,3-difluorobenzene (0.10 M) with LDA (0.12 M) in neat THF at  $-78\text{ }^\circ\text{C}$ : (A) no added LiCl; (B) 0.5 mol% LiCl; (C) 0.5 and 10 mol% LiCl.

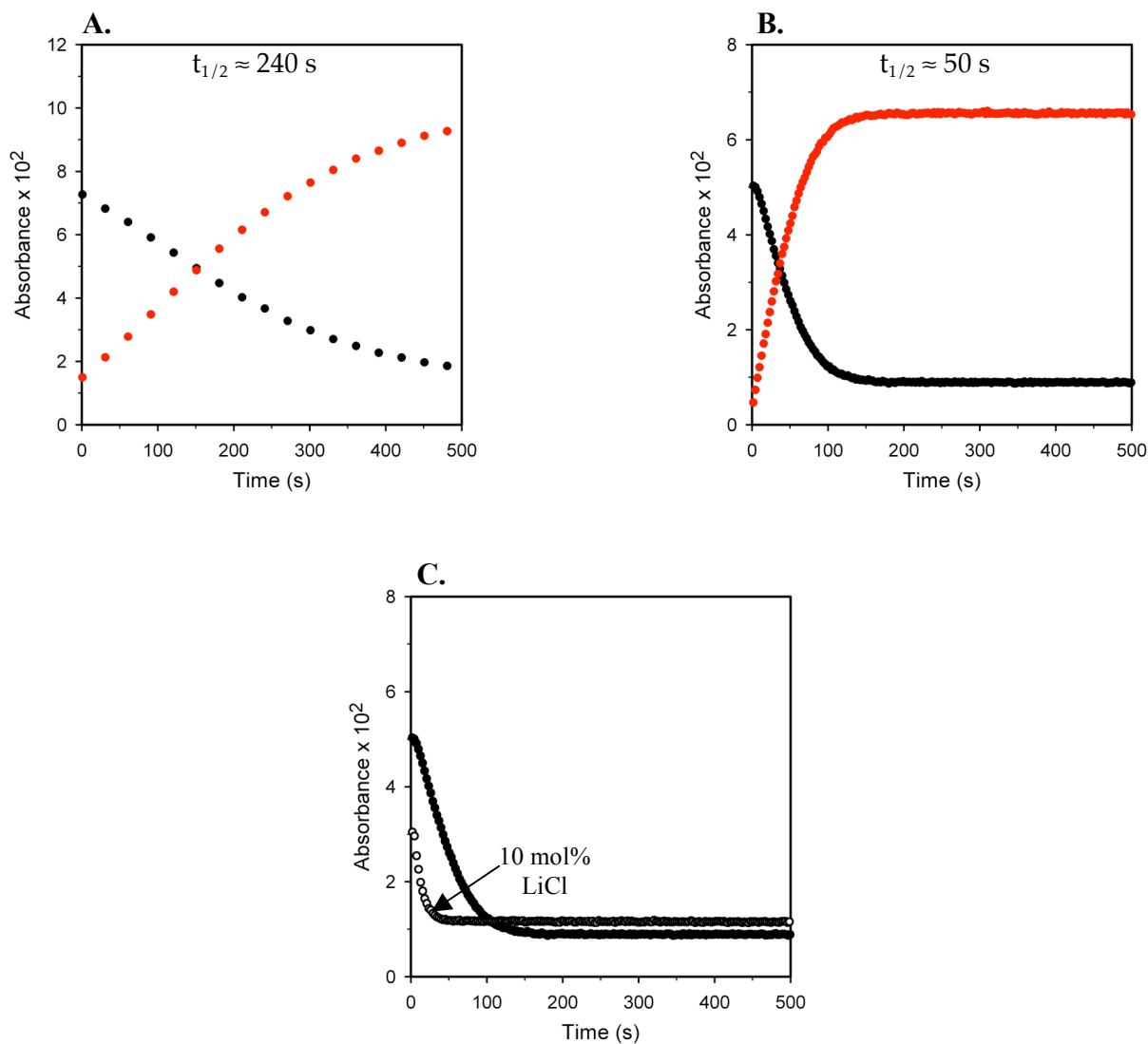
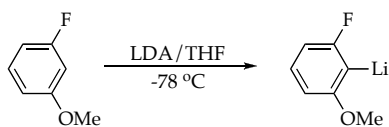




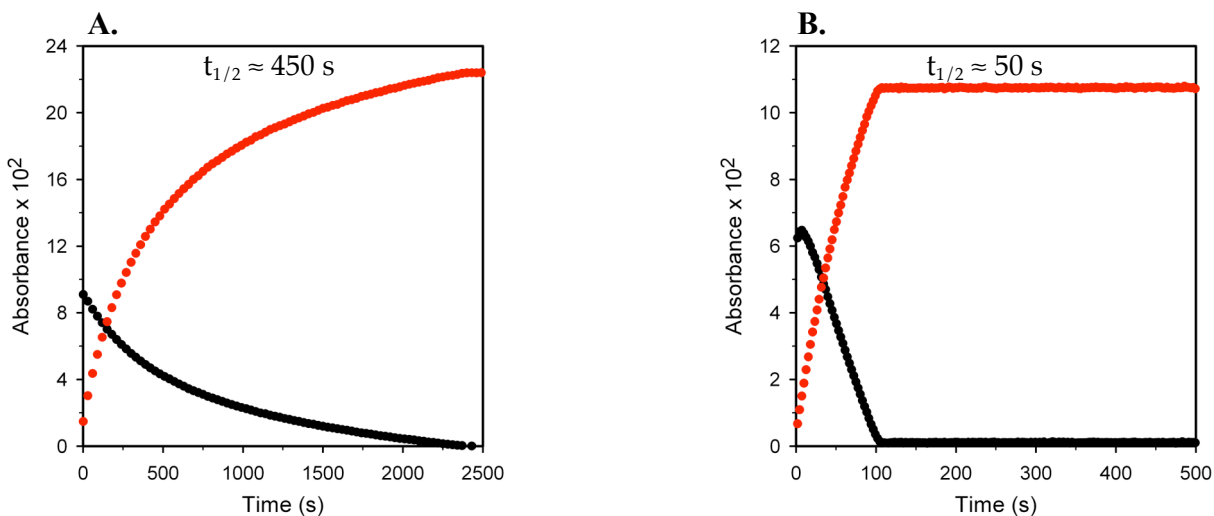
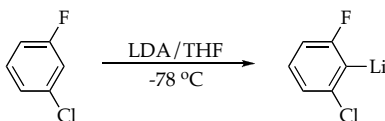
**III.** Plot of IR absorbances (black –  $1715\text{ cm}^{-1}$ , red –  $1657\text{ cm}^{-1}$ ) versus time for the ortholithiation of 3-fluorophenyl-*N,N*-diisopropylcarbamate (0.10 M) with LDA (0.12 M) in neat THF at  $-78\text{ }^\circ\text{C}$ : (A) no added LiCl; (B) 0.5 mol% LiCl.



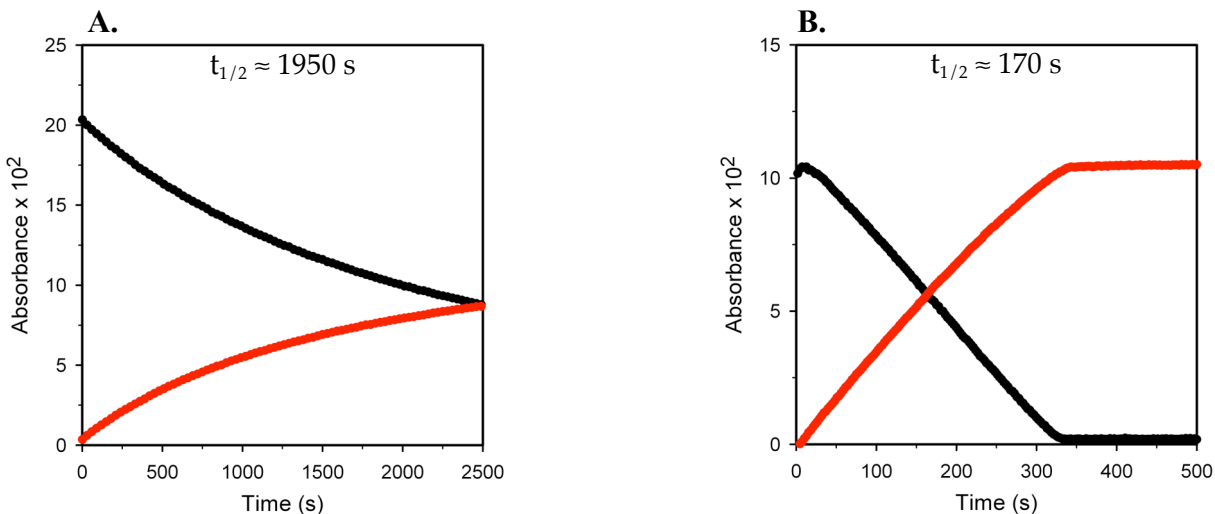
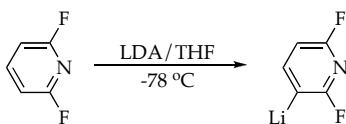
IV. Plot of IR absorbances (black –  $1721\text{ cm}^{-1}$ , red –  $1661\text{ cm}^{-1}$ ) versus time for the ortholithiation of 1,3-bis(*N,N*-diisopropylcarbamoyl)benzene (0.10 M) with LDA (0.12 M) in neat THF at  $-78\text{ }^\circ\text{C}$ : (A) no added LiCl; (B) 0.5 mol% LiCl; (C) 0.5 and 10 mol% LiCl.



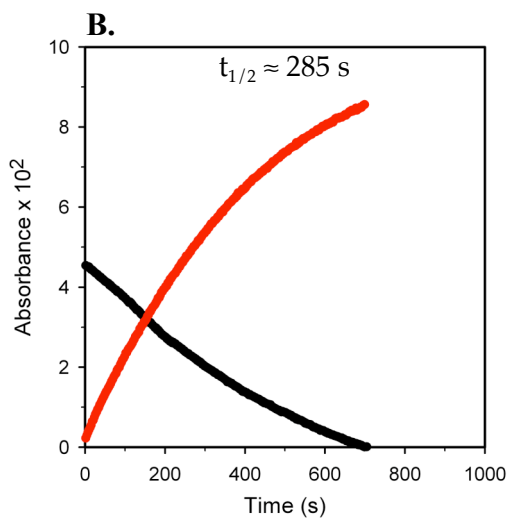
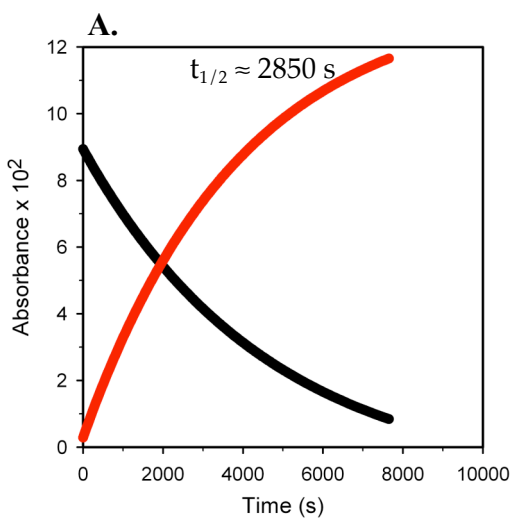
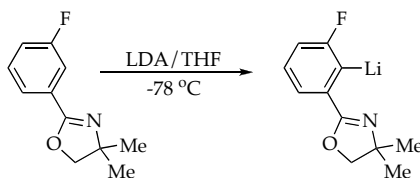
V. Plot of IR absorbances (black –  $1617\text{ cm}^{-1}$ , red –  $1412\text{ cm}^{-1}$ ) versus time for the ortholithiation of 3-fluoroanisole (0.10 M) with LDA (0.12 M) in neat THF at  $-78\text{ }^\circ\text{C}$ : (A) no added LiCl; (B) 0.5 mol% LiCl (C) 0.5 and 10 mol% LiCl.



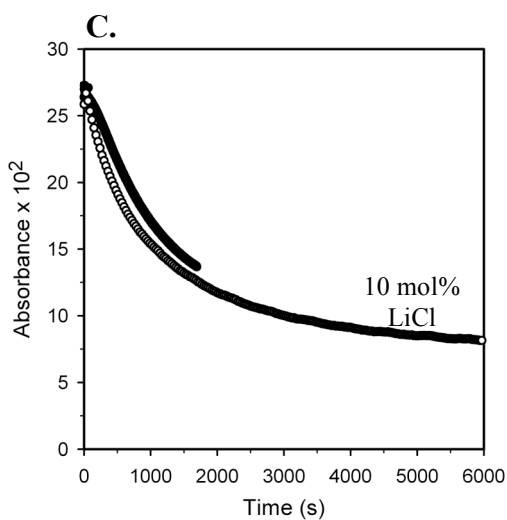
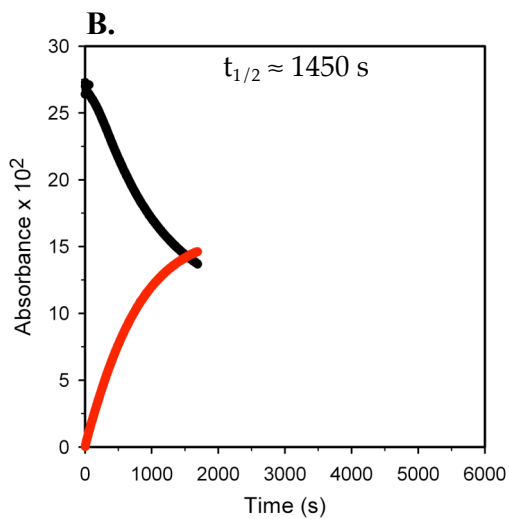
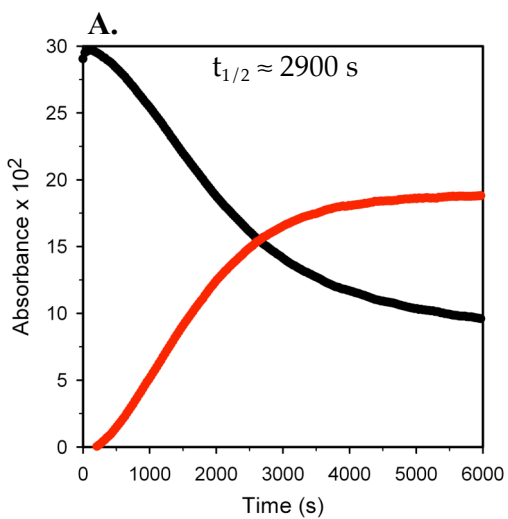
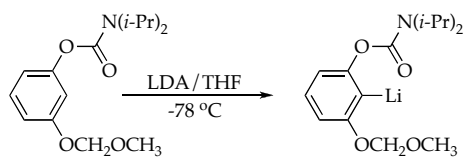
VI. Plot of IR absorbances (black –  $1595\text{ cm}^{-1}$ , red –  $1397\text{ cm}^{-1}$ ) versus time for the ortholithiation of 1-chloro-3-fluorobenzene (0.10 M) with LDA (0.12 M) in neat THF at  $-78\text{ }^\circ\text{C}$ : (A) no added LiCl; (B) 0.5 mol% LiCl.



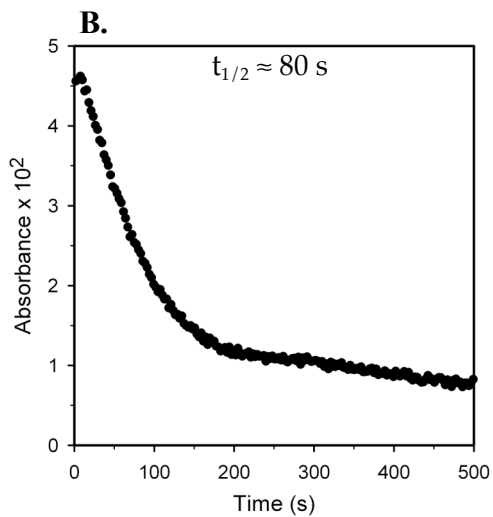
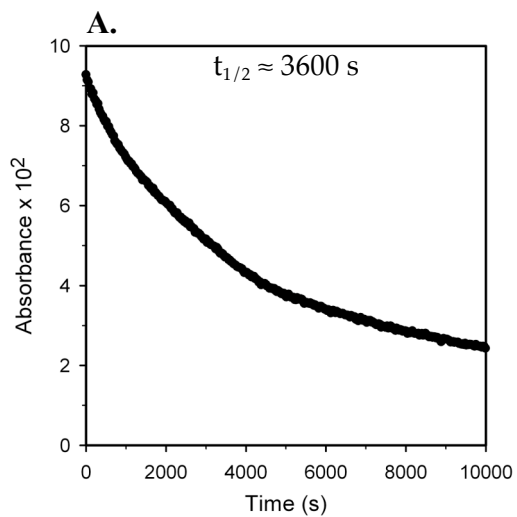
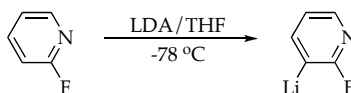
VII. Plot of IR absorbances (black –  $1610\text{ cm}^{-1}$ , red –  $1514\text{ cm}^{-1}$ ) versus time for the ortholithiation of 2,6-difluoropyridine (0.10 M) with LDA (0.12 M) in neat THF at  $-78\text{ }^\circ\text{C}$ : (A) no added LiCl; (B) 0.5 mol% LiCl.



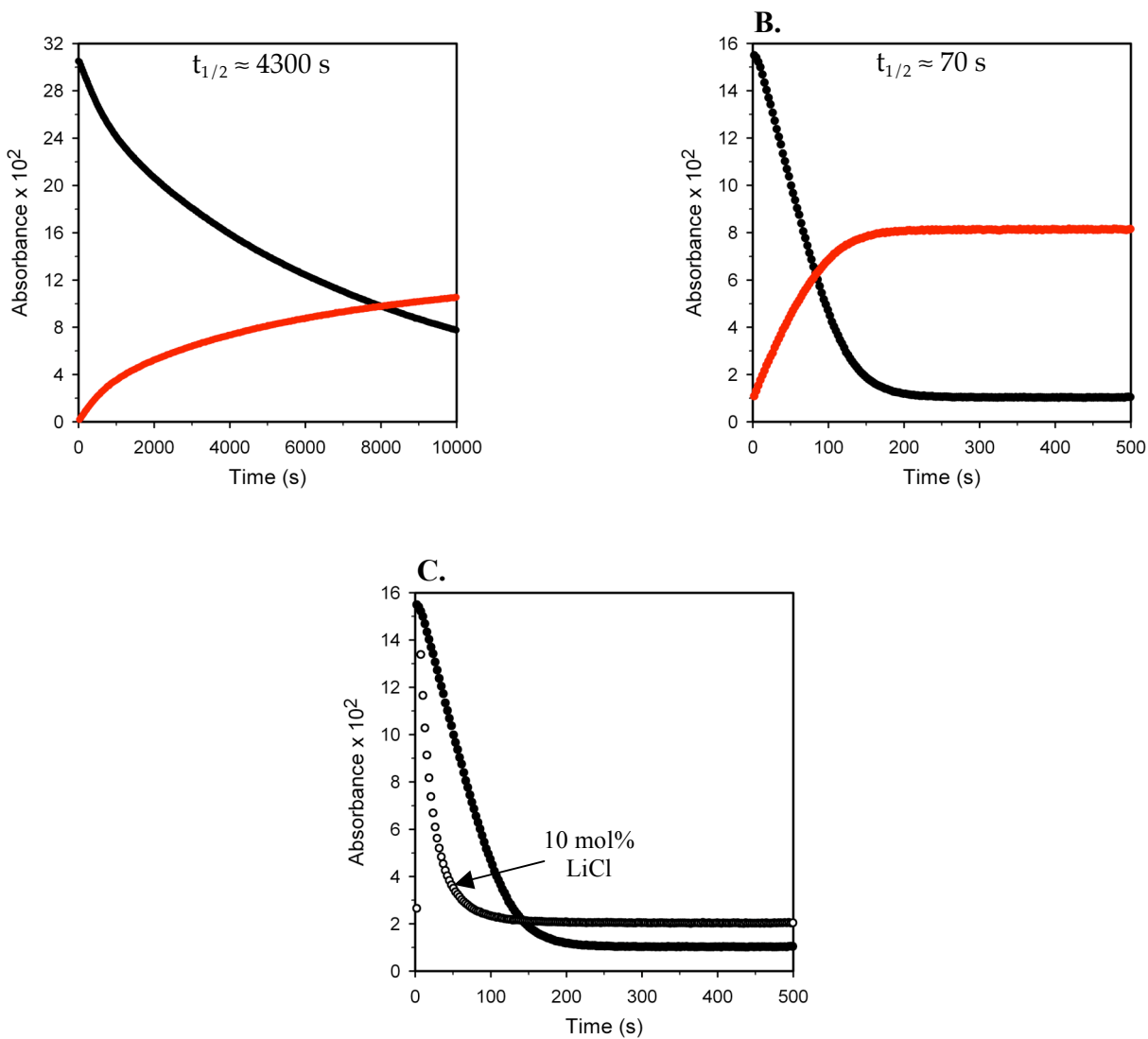
**VIII.** Plot of IR absorbances (black – 1653  $\text{cm}^{-1}$ , red – 1622  $\text{cm}^{-1}$ ) versus time for the ortholithiation of 2-(3-fluorophenyl)-4,4-dimethyl-4,5-dihydro-1,3-oxazole (0.10 M) with LDA (0.12 M) in neat THF at  $-78\text{ }^{\circ}\text{C}$ : (A) no added LiCl; (B) 0.5 mol% LiCl.



IX. Plot of IR absorbances (black –  $1719\text{ cm}^{-1}$ , red –  $1659\text{ cm}^{-1}$ ) versus time for the ortholithiation of 3-methoxymethoxyphenyl-*N,N*-diisopropylcarbamate (0.10 M) with LDA (0.12 M) in neat THF at  $-78\text{ }^\circ\text{C}$ : (A) no added LiCl; (B) 0.5 mol% LiCl; (C) 0.5 and 10 mol% LiCl.

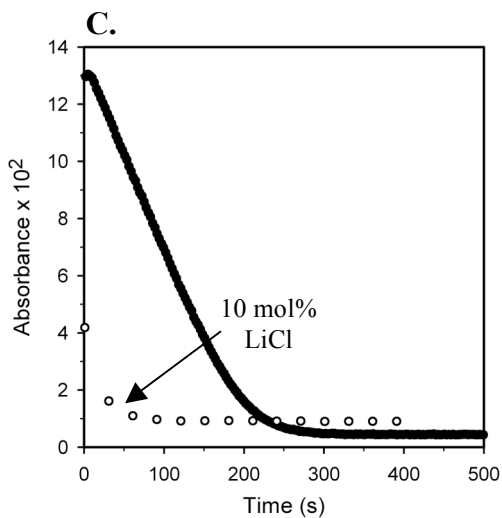
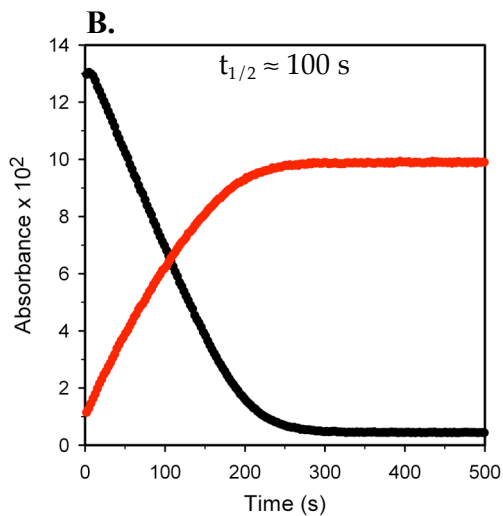
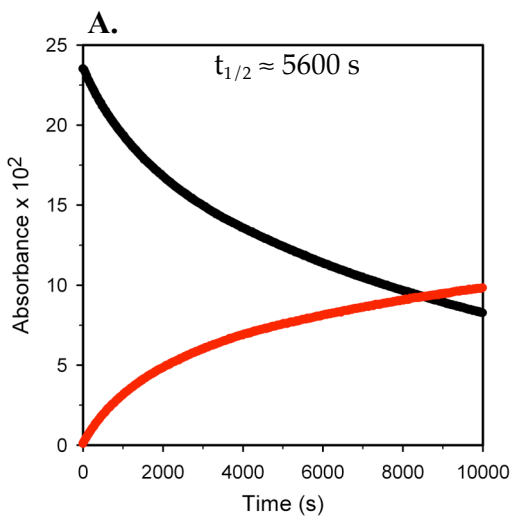
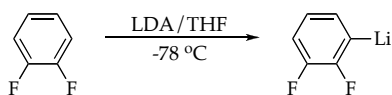


**X.** Plot of IR absorbances (black – 1597 cm<sup>-1</sup>) versus time for the ortholithiation of 2-fluoropyridine (0.10 M) with LDA (0.12 M) in neat THF at -78 °C: (A) no added LiCl; (B) 0.5 mol% LiCl.

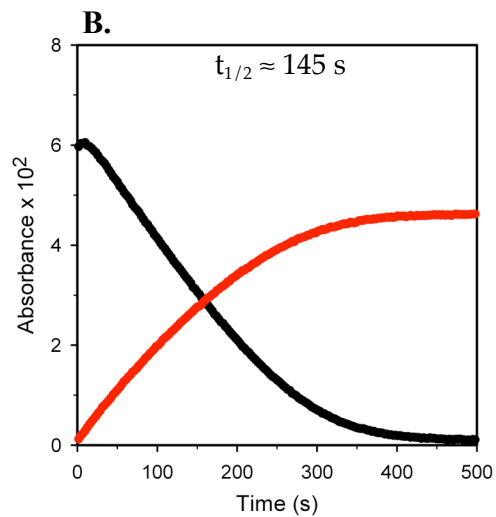
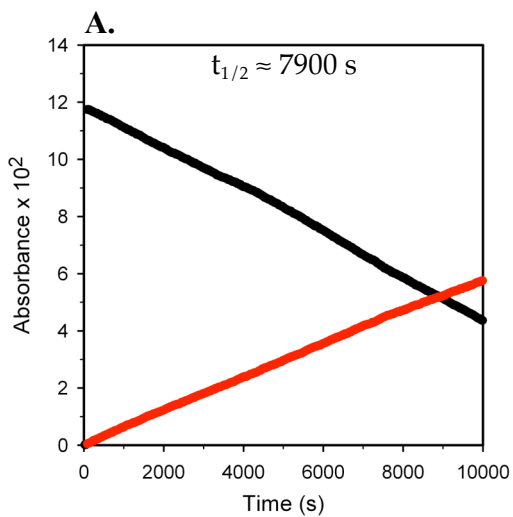
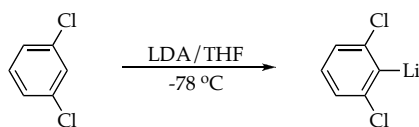


XI. Plot of IR absorbances (black –  $1507\text{ cm}^{-1}$ , red –  $1418\text{ cm}^{-1}$ ) versus time for the ortholithiation of 1,4-difluorobenzene (0.10 M) with LDA (0.12 M) in neat THF at  $-78\text{ }^\circ\text{C}$ : (A) no added LiCl; (B) 0.5 mol% LiCl; (C) 0.5 and 10 mol% LiCl.

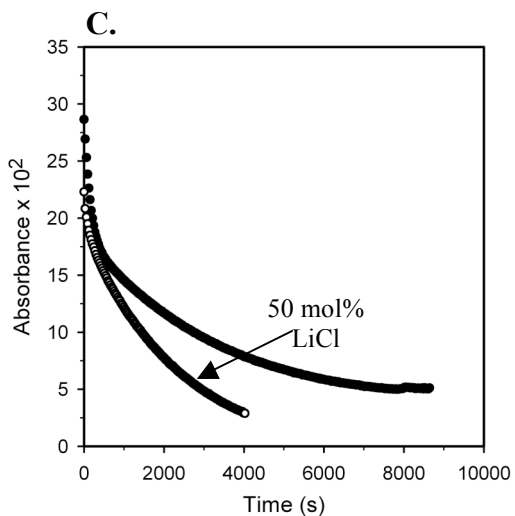
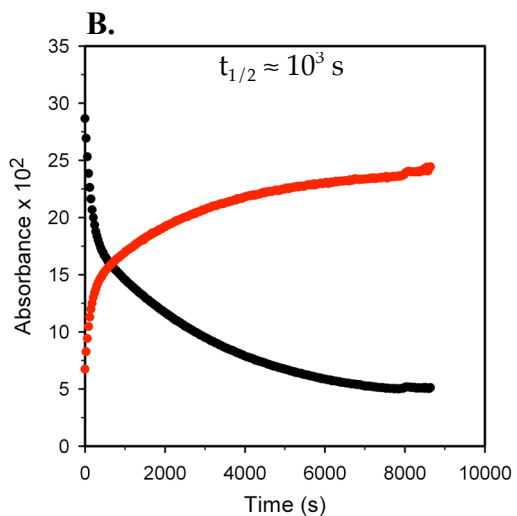
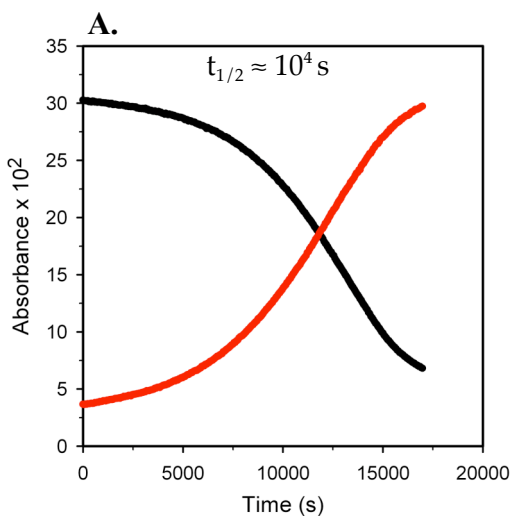
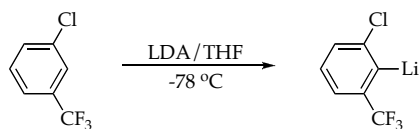




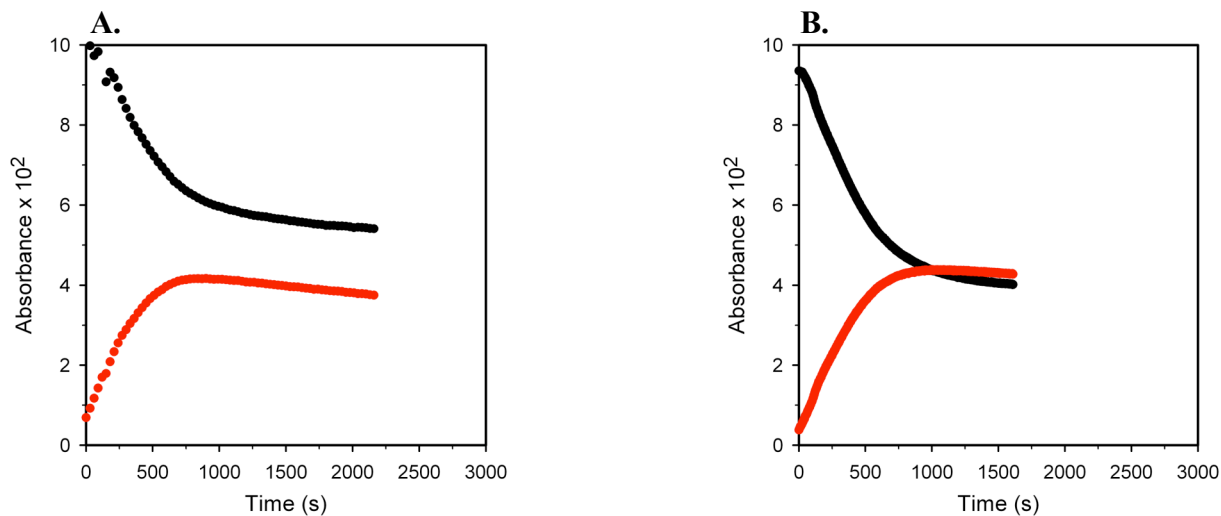
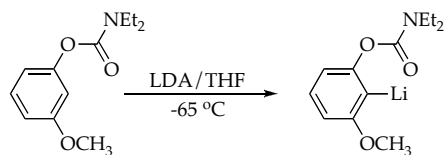
**XII.** Plot of IR absorbances (black – 1509  $\text{cm}^{-1}$ , red – 1391  $\text{cm}^{-1}$ ) versus time for the ortholithiation of 1,2-difluorobenzene (0.10 M) with LDA (0.12 M) in neat THF at  $-78\text{ }^\circ\text{C}$ : (A) no added LiCl; (B) 0.5 mol% LiCl; (C) 0.5 and 10 mol% LiCl.



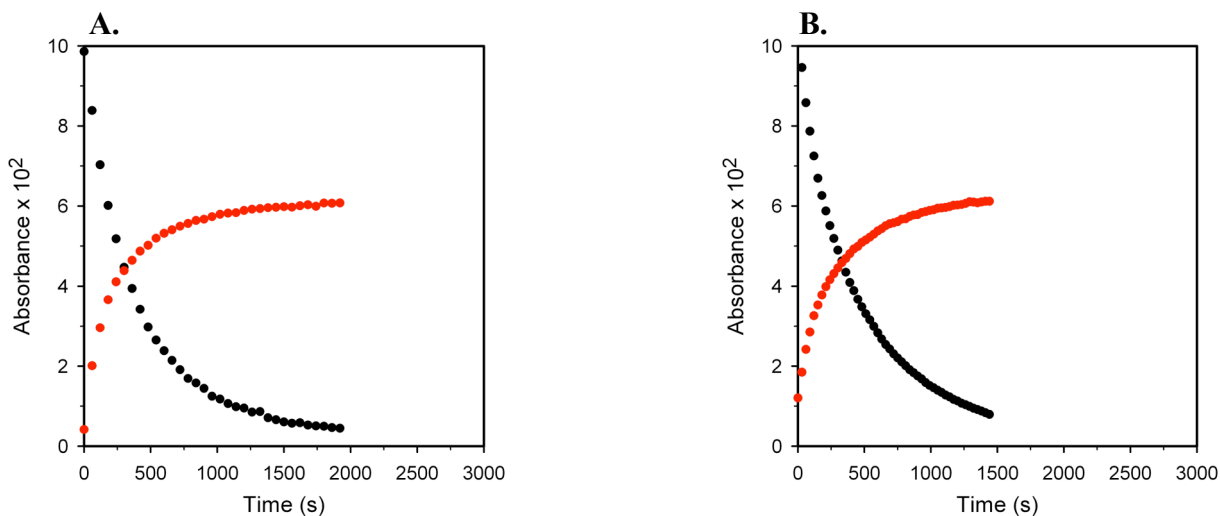
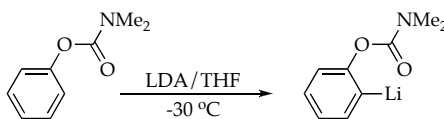
**XIII.** Plot of IR absorbances (black – 1576  $\text{cm}^{-1}$ , red – 1534  $\text{cm}^{-1}$ ) versus time for the ortholithiation of 1,3-dichlorobenzene (0.10 M) with LDA (0.12 M) in neat THF at -78  $^\circ\text{C}$ : (A) no added LiCl; (B) 0.5 mol% LiCl.



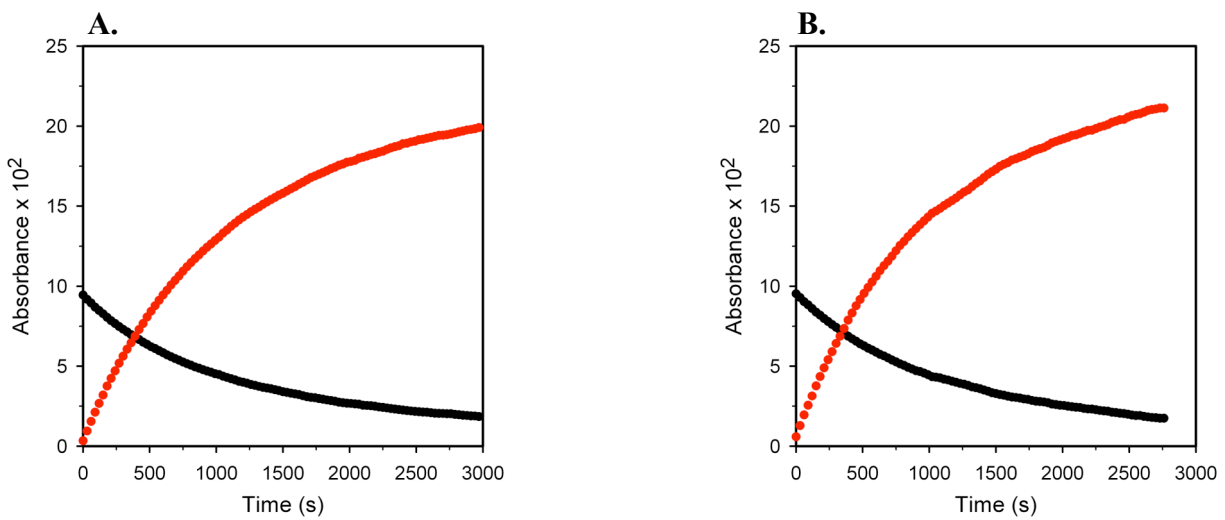
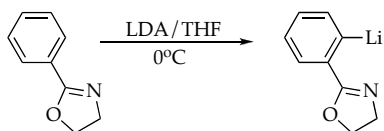
**XIV.** Plot of IR absorbances (black –  $1326 \text{ cm}^{-1}$ , red –  $1306 \text{ cm}^{-1}$ ) versus time for the ortholithiation of 3-chlorobenzotrifluoride (0.10 M) with LDA (0.12 M) in neat THF at  $-78\text{ }^\circ\text{C}$ : (A) no added LiCl; (B) 0.5 mol% LiCl; (C) 0.5 and 50 mol% LiCl.



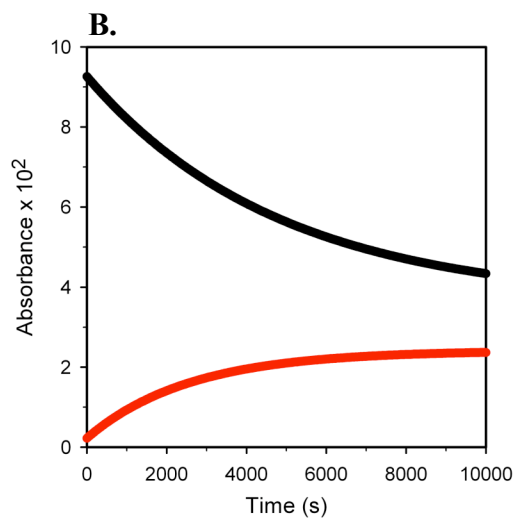
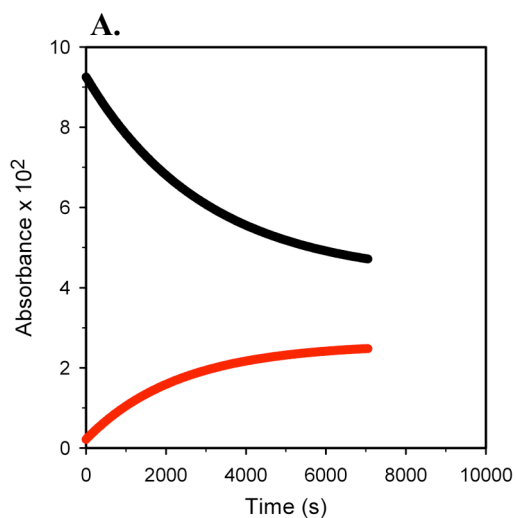
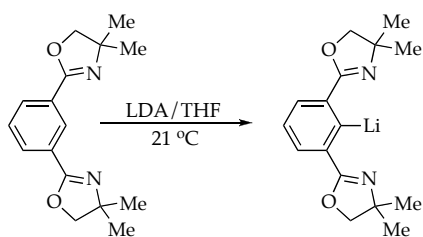
XV. Plot of IR absorbances (black –  $1725\text{ cm}^{-1}$ , red –  $1675\text{ cm}^{-1}$ ) versus time for the ortholithiation of 3-methoxyphenyl-*N,N*-diethylcarbamate (0.10 M) with LDA (0.12 M) in neat THF at  $-65\text{ }^{\circ}\text{C}$ : (A) no added LiCl; (B) 0.5 mol% LiCl.



XVI. Plot of IR absorbances (black –  $1725\text{ cm}^{-1}$ , red –  $1675\text{ cm}^{-1}$ ) versus time for the ortholithiation of phenyl-*N,N*-dimethylcarbamate (0.10 M) with LDA (0.12 M) in neat THF at  $-30\text{ }^{\circ}\text{C}$ : (A) no added LiCl; (B) 0.5 mol% LiCl.

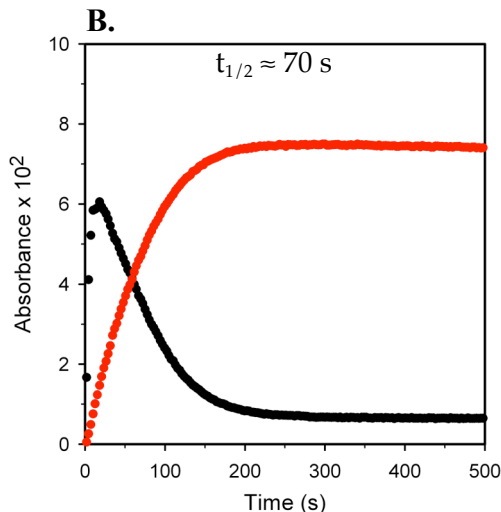
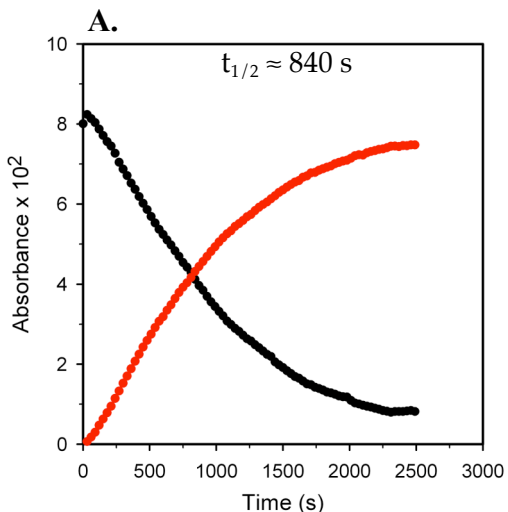
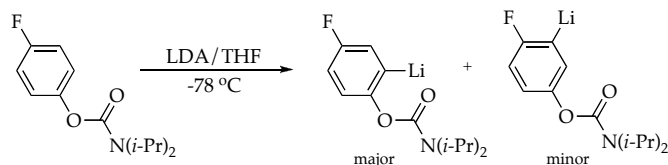


**XVII.** Plot of IR absorbances (black – 1652 cm<sup>-1</sup>, red – 1526 cm<sup>-1</sup>) versus time for the ortholithiation of 2-phenyl-2-oxazoline (0.10 M) with LDA (0.12 M) in neat THF at 0 °C: (A) no added LiCl; (B) 0.5 mol% LiCl.

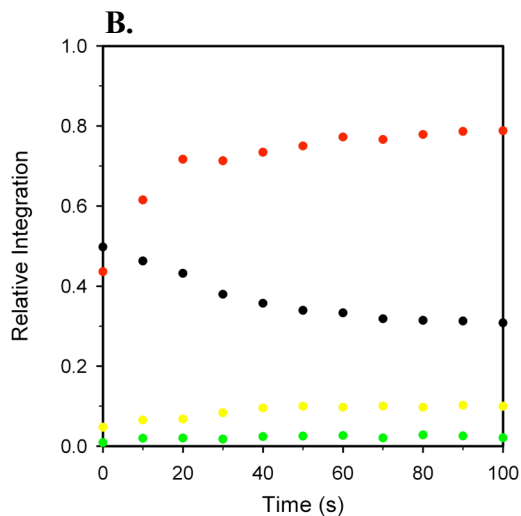
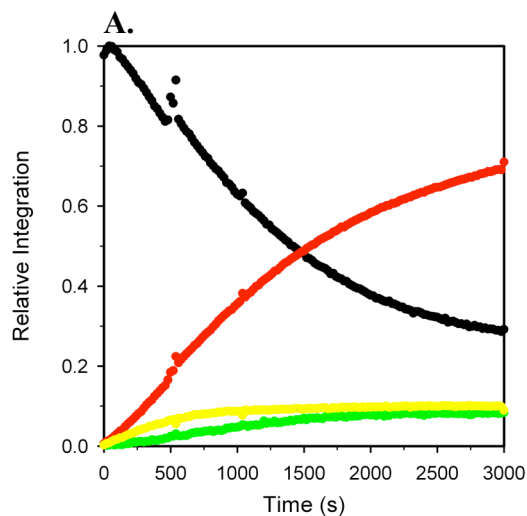


**XVIII.** Plot of IR absorbances (black – 1654  $\text{cm}^{-1}$ , red – 1520  $\text{cm}^{-1}$ ) versus time for the ortholithiation of 1,3-bis(4',4'-dimethyl-2'-oxazoliny)benzene (0.10 M) with LDA (0.12 M) in neat THF at 21 °C: (A) no added LiCl; (B) 0.5 mol% LiCl.



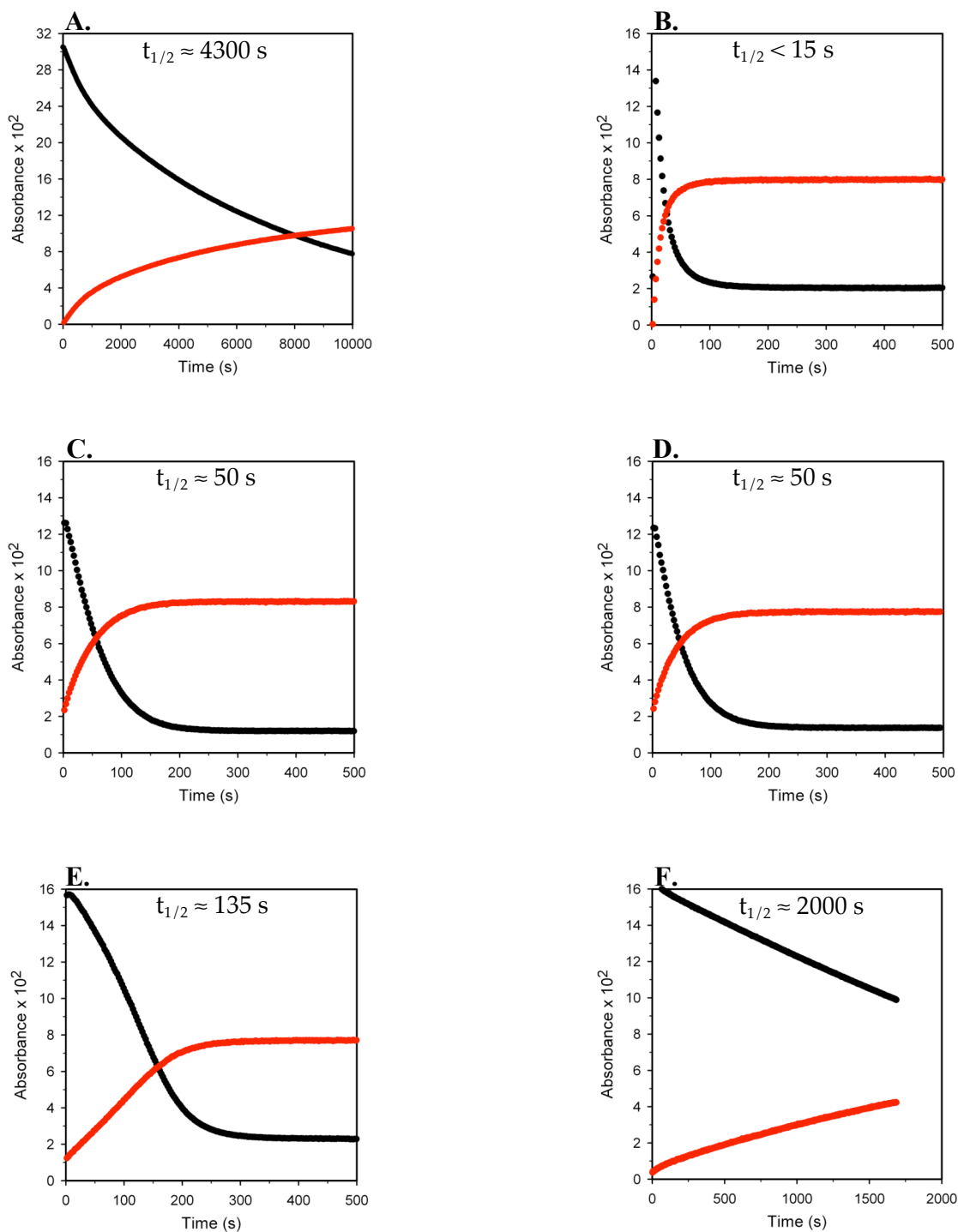


**XXI.** Plot of IR absorbances (black –  $1717\text{ cm}^{-1}$ , red –  $1657\text{ cm}^{-1}$ ) versus time for the ortholithiation of 4-fluorophenyl-*N,N*-diisopropylcarbamate (0.025 M) with LDA (0.12 M) in neat THF at  $-78\text{ }^\circ\text{C}$ : (A) no added LiCl; (B) 0.5 mol% LiCl.

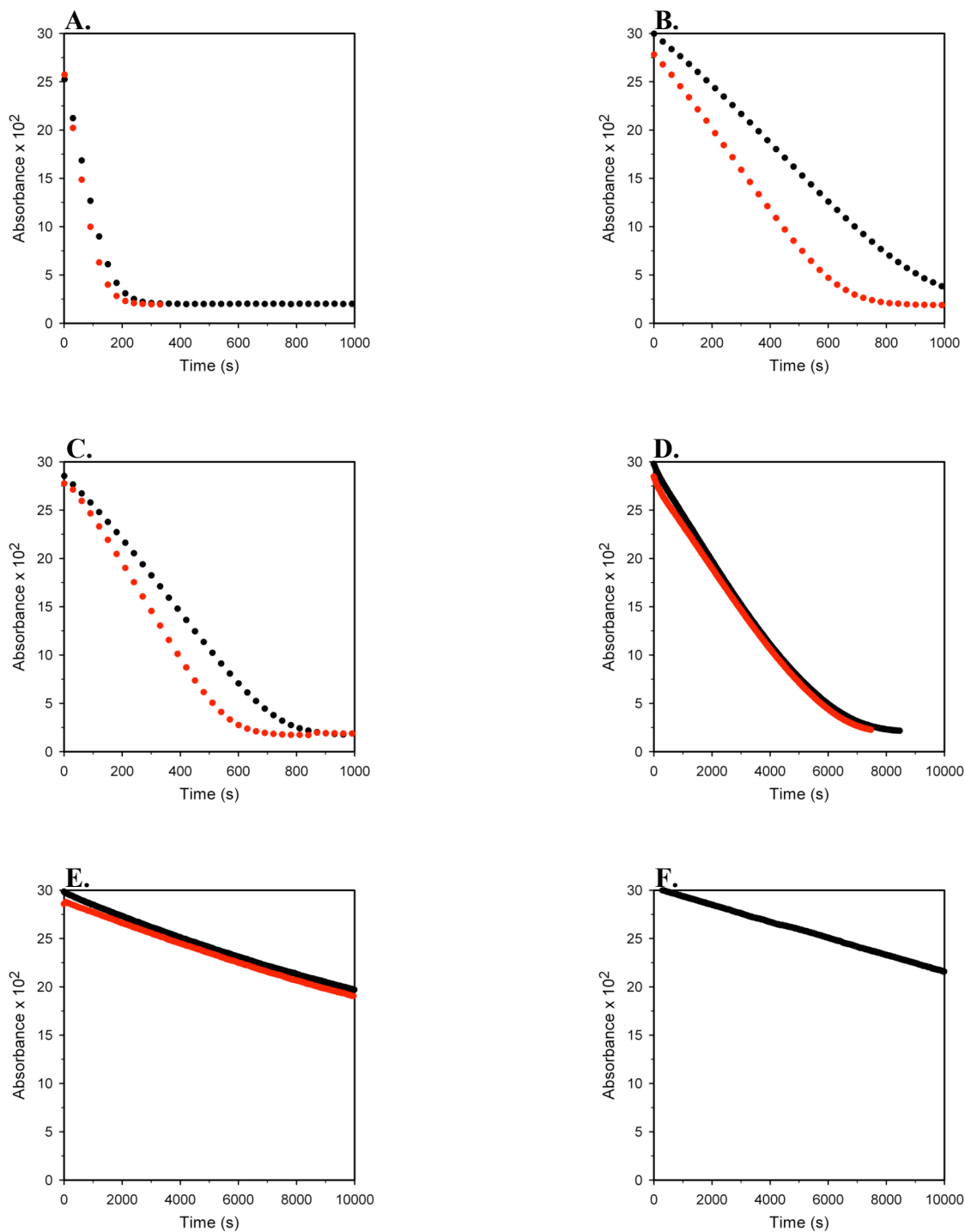


**XXII.** Plot of  $^{19}\text{F}$  NMR peak integrations (black:  $\delta$  -118.8, red:  $\delta$  -123.7, green:  $\delta$  85.5, yellow:  $\delta$  -124.1) versus time for the ortholithiation of 4-fluorophenyl-*N,N*-diisopropylcarbamate (0.05 M) with LDA (0.20 M) in neat THF at  $-78\text{ }^\circ\text{C}$ : (A) no added LiCl; (B) 10 mol% LiCl.





**XXIII.** Plot of IR absorbances (black – 1507  $\text{cm}^{-1}$ , red – 1418  $\text{cm}^{-1}$ ) versus time for the ortholithiation of 1,4-difluorobenzene (0.10 M) with LDA (0.12 M) in neat THF at  $-78$   $^{\circ}\text{C}$ : (A) no additive; (B) 10 mol% LiCl; (C) 10 mol% LiBr; (D) 10 mol% PhCCl<sub>2</sub>; (E) 10 mol% PhCOOLi; (F) 10 mol% PhOLi.



**XXIV.** Plot of IR absorbances (black/red – duplicated rates) versus time for the ortholithiation of 1,4-difluorobenzene (0.10 M) with LDA (0.12 M) in 10.0 M THF/hexane at -78 °C using: (A) Acros *n*-BuLi – batch1; (B) Acros *n*-BuLi – batch2; (C) Aldrich *n*-BuLi – batch1; (D) Aldrich *n*-BuLi – batch2; (E) Acros LDA; (F) Aldrich LDA